Materials Sciences and Applications, 2012, 3, 861-871
http://dx.doi.org/10.4236/msa.2012.312126 Published Online December 2012 (http://www.SciRP.org/journal/msa)

FP-LMTO Calculations of Structural and Electronic Properties of Alkaline-Earth Chalcogenides Alloys AY: A = Ca, Sr, Ba; Y = S

Mohammed Ameri[1*], Keltouma Boudia[1], Abbes Rabhi[2], Samir Benaissa[3], Yarub Al-Douri[4], Abdelmadjid Rais[1], Djelloul Hachemane[1]

[1]Department of Physics, University Djillali Liabes, Sidi Bel Abbes, Algeria; [2]Department of Mathematics, University of Sidi Bel Abbes, Sidi Bel Abbes, Algeria; [3]Laboratory of Statistics and Stochastic Processes, University Djillali Liabes, Sidi Bel Abbes, Algeria; [4]Nono Institute of Electronic Engineering, University Malaysia Perlis, Kangar, Malaysia
Email: [*]lttnsameri@yahoo.fr.

Received August 28th, 2012; revised September 27th, 2012; accepted October 26th, 2012

ABSTRACT

The structural and the electronic properties of the ternary $Sr_xCa_{1-x}S$, $Ba_xCa_{1-x}S$ and $Ba_xSr_{1-x}S$ alloys have been calculated using the full-potential linear muffin-tin-orbital (FP-LMTO) method based on density functional theory, within both local density approximation (LDA) and generalized gradient approximation (GGA). The calculated equilibrium lattice constants and bulk modulus are compared with previous results. The concentration dependence of the electronic band structure and the direct and indirect band gaps are investigated. Using the approach of Zunger and co-workers, the microscopic origins of the band gap bowing are investigated also. A reason is found from the comparison of our results with other theoretical calculations.

Keywords: SrS; BaS; CaS; Semiconductors; FP-LMTO; Alloys; Bowing Parameter

1. Introduction

The II-VI compound semiconductors (AY: A = Ca, Sr, Ba; Y = S) have recently received considerable interest from the blue to the near-ultraviolet spectral region of both experimental and theoretical points of view [1]. This was due to their potential technological applications, in light-emitting diodes (LEDs) and laser diodes (LDs) [2]. Many experimental and theoretical works were reported for II-VI chalcogenides, calcium chalcogenides [3,4], strontium chalcogenides, and beryllium chalcogenides [5]. The alkaline earth chalcogenides form a closed-shell ionic system crystallized in the rocksalt type structure-type (B1) at ambient conditions. They are technologically important materials, with applications in the area of luminescent devices, radiation dosimetry, fast high-resolution optically stimulated luminescence imaging, and infrared sensitive devices [6-8]. Group II-VI semiconductors and their heterostructures are well known to form ternary alloys with a direct fundamental band gap over most of the alloy composition range with high absorption coefficients. They are used as which can be used as materials for fabricating thin film heterojunction photovoltaic (PV) devices. The principal energy gaps of ternary II-VI semiconductor alloys can cover various light spectra over the entire composition, and lattice parameters can be tailored independently to fabricate photovoltaic devices on suitable lattice matched substrates [9]. The use of II-VI semiconductor alloys for device applications requires: better controlling of the process conditions and parameters during the material growth and device fabrication, reliable and accurate modeling simulation of structural and electronic properties of heterostructures as a function of interface strain and composition [10]. The principal energy gaps of ternary II-VI semiconductor alloys can cover various light spectra over the entire composition, and lattice parameters can be tailored independently to fabricate photovoltaic devices on suitable lattice matched substrates [11]. Therefore, the goal of this work is to calculate the structural and the electronic properties by using the full-potential linear muffin-tin-orbital (FP-LMTO) method within the local density approximation (LDA), and two newly developed refinements, named the generalized gradient approximation (GGA) of Perdew *et al*. The physical origins of gap bowing are calculated following the approach of Zunger *et al.* (and workers) [12]. In this approach, the alloys are is studied in an ordered structure (we use here a cubic

[*]Corresponding author.

super cell of eight atoms) designed to reproduce the most important pair-correlation functions of random disordered alloys and where the chemical and structural effects are captured very well. The paper is organized as follows. The computational method that we have adopted for the calculation is described in Section 2. We present our results in Section 3. Finally, conclusions are given in Section 4.

2. Method of Calculations

The calculations reported here were carried out using the *ab-initio* full-potential linear muffin-tin orbital (FP-LMTO) method [13-16] as implemented in the Lmtart code [17]. The exchange and correlation potential were calculated using the local density approximation (LDA) [18] and the generalized approximation (GGA) [19]. This is an improved method compared to previous (LMTO) methods. The FP-LMTO method treats muffin-tin spheres and interstitial regions on the same footing, leading to improvements in the precision of the eingen-values. At the same time, the FP-LMTO method, in which the space is divided into an interstitial regions (IR) and non overlapping muffin-tin spheres (MTS) surrounding the atomic sites use more complete basis than its predecessors. The space in this method is divided into non-overlapping muffin-tin (MT) spheres centered at the atomic sites separated by an interstitial region (IR). In the IR regions, the basis set consists of plane waves. Inside the MT spheres, the basis sets is described by radial solutions of the one particle Schrödinger equation (at fixed energy) and their energy derivatives multiplied by spherical harmonics. The charge density and the potential are represented inside the MTS by spherical harmonics up to $l_{max} = 6$. The integrals over the Brillouin zone are performed up to 35 special *k*-points for binary compounds and 27 special *k*-points for the alloys in the ireducible Brillouin zone (IBZ), using the Blöchl's modified tetrahedron method [20]. The self-consistent calculations are considered to be converged when the total energy of the system is stable within 10^{-5} Ry. In order to avoid the overlap of atomic spheres, the MTS radius for each atomic position is taken to be different for each composition. We point out that the use of the full-potential calculation ensures that the calculation is not completely independent of the choice of sphere radii. Both plane waves cut-off are varied to ensure the total energy convergence. The values of the sphere radii (MTS) number of plane waves (NPLW), used in our calculation are summarized in **Table 1**.

3. Results and Discussions

3.1. Structural Properties

The structural properties of CaS, SrS and BaS binary compounds and their $Sr_xCa_{1-x}S$, $Ba_xCa_{1-x}S$, $Ba_xSr_{1-x}S$ alloys in the cubic structure by means of the full-potential LMTO method are calculated. As for the ternary semiconductor alloys with the type of $B_xA_{1-x}C$, we have started our FP-LMTO calculations of the structural properties with the rocksalt structure and let the calculation

Table 1. (a) The plane wave number PW, energy cut- off (in Ry) and the muffin-tin radius (MTS) (in a.u.) used in calculation for binary SrS and CaS and their $Sr_xCa_{1-x}S$, $Ba_xCa_{1-x}S$, $Ba_xSr_{1-x}S$, alloy in the rocksalt structure (B1);(b) binary BaS and CaS and their $Ba_xCa_{1-x}S$ alloy in in the rocksalt structure (B1); (c) binary BaS and CaS and their $Ba_xSr_{1-x}S$ alloy in in the rocksalt structure (B1).

(a)

x	PW		E_{cut} total (Ry)		MTS (a.u)	
	LDA	GGA	LDA	GGA	LDA	GGA
0	2974	6566	64.468	109.273	Ca 2.932	2.932
					S 2.60	2.60
0.25	17076	33400	82.1554	128.367	Ca 3.158	3.158
					Sr 3.158	3.158
					S 2.748	2.748
0.50	20478	38910	90.378	137.912	Ca 3.060	3.060
					Sr 3.060	3.060
					S 2.663	2.663
0.75	24404	50882	99.571	162.570	Ca 2.847	2.847
					Sr 2.856	2.856
					S 2.557	2.557
1	2974	6566	60.939	103.292	Sr 3.073	3.073
					S 2.618	2.618

(b)

	PW	E_{cut} total (Ry)	MTS (a.u)
x	LDA GGA	LDA GGA	LDA GGA
0	2974 6566	64.468 109.273	Ca 2.932 2.932 S 2.60 2.600
0.25	20478 44472	90.312 151.249	Ca 2.978 2.978 Ba 3.030 3.030 S 2.602 2.602
0.50	20478 44472	85.314 142.878	Ca 3.117 3.117 Ba 3.117 3.117 S 2.664 2.664
0.75	20478 44472	81.364 136.263	Ca.192 3.192 Ba3.213 3.213 S 2.680 2.680
1	2974 6566	53.812 91.211	Ba 3.331 3.331 S 2.725 2.725

(c)

	PW	E_{cut} total (Ry)	MTS (a.u)
x	LDA GGA	LDA GGA	LDA GGA
0	2974 6566	60.939 103.292	Sr 3.073 3.073 S 2.618 2.618
0.25	20478 44472	85.337 142.917	Sr 3.121 3.121 Ba 3.148 3.148 S 2.639 2.639
0.50	20478 44472	82.898 138.8324	Sr 3.194 3.117 Ba 3.194 3.117 S 2.671 2.664
0.75	20478 44472	80.237 134.375	Sr 3.246 3.246 Ba 3.257 3.257 S 2.691 2.691
1	2974 6566	53.812 91.211	Ba 3.331 3.331 S 2.725 2.725

forces move the atoms to their equilibrium positions. We have chosen the basic cubic cell as the unit cell. In the unit cell, there are four C anions, three A and one B, two A and two B, one A and three B cations, for x = 0.25, 0.50 and 0.75, respectively. For the considered structures, we have performed the structural optimization by calculating the total energies for different volumes around the equilibrium cell volume V_0 of CaS, SrS and BaS binary compounds and their alloys. The calculated total energies are fitted to the Murnaghan's equation of state [21] to determine the ground state properties such as the equilibrium lattice constant a and the bulk modulus B. The calculated equilibrium parameters (a and B) are given in **Table 2** that also contains results of previous calculations as well as the available experimental data. As a whole, our calculated structural parameters are in good agreement with those obtained by first-principles methods within different approximations. The calculated lattice parameter for CaS, SrS and BaS binary compound is in good agreement with other data, which ensures the reliability of the present first-principles computations. The computed lattice parameter slightly underestimates and overestimates the other data by using LDA and GGA, respectively, which are consistent with the general trend of these approximations. As it can be seen, the calculated lattice parameter for BaS is larger than those of SrS and CaS. As the anion atom is the same in the compounds, this result can be easily explained by considering the

Table 2. Calculated lattice parameter *a* and bulk modulus *B* compared to experimental and other theoretical results of CaS, SrS and BaS and their $Sr_xCa_{1-x}S$, $Ba_xCa_{1-x}S$ and $Ba_xSr_{1-x}S$ alloys in the rocksalt structure (B1).

Compounds	Lattice constant a (Å)	Bulk modulus *B* (GPa)
SrS		
LDA	5.868	61.383
GGA	6.023	51.103
Expt	6.024[a]	58[a]
Others	6.067[a], 5.774[h], 6.07[a], 6.065[g]	47[b], 62[h],
CaS		
LDA	5.689	87.228
GGA	5.856	61.236
Expt	5.689[g]	64[g]
Others	5.64[i], 5.645[i] ,5.69[j], 5.598[c], 5.721[d], 5.717[e]	65.2[c], 57[d], 57.42[e]
BaS		
LDA	6.196	46.257
GGA	6.41	37.299
Others		42.36[f], 52.46[g]
Expt	6.38[l]	39.42[f]
$Sr_{0.25}Ca_{0.75}S$		
LDA	5.717	87.228
GGA	5.869	61.236
Others	5.83[k] , 5.98[kk]	60.26[k], 48.94[k]
$Sr_{0.5}Ca_{0.5}S$		
LDA	5.788	67.403
GGA	5.946	
Others	5.757[k], 5.903[k]	62.91[k], 52.413[k]
$Sr_{0.75}Ca_{0.25}S$		67.991
LDA	5.801	76.068
GGA	5.959	58.299
Others	5.66[k] 5.815[k]	65.63[k], 54.815[k]
$Ba_{0.25}Ca_{0.75}S$		
LDA	5.775	75.627
GGA	5.948	57.124
$Ba_{0.5}Ca_{0.5}S$		68.578
LDA	5.963	
GGA	6.120	52.278
$Ba_{0.75}Ca_{0.25}S$		
LDA	6.094	69.459
GGA	6.266	49.488
$Ba_{0.25}Sr_{0.75}S$		
LDA	5.937	81.796
GGA	6.119	57.271
$Ba_{0.5}Sr_{0.5}S$		
LDA	6.027	78.123
GGA	6.208	55.215
$Ba_{0.75}Sr_{0.25}S$		
LDA	6.1369	68.725
GGA	6.310	49.341

[a]Ref [33]; [b]Ref. [34]; [c]Ref. [35]; [d]Ref. [36]; [e]Ref. [37]; [f]Ref. [38]; [g]Ref. [39]; [h]Ref. [40]; [i]Ref. [41]; [J]Ref. [42]; [k]Ref. [43]; [l]Ref. [44].

atomic radii of Ca, Sr, and Ba: R(Ca) = 1.80 Å, R(Sr) = 2.00 Å, R(Ba) = 2.15 Å; *i.e.* the lattice constant increases with increasing atomic size of the cation element. The bulk modulus value for CaS is larger than those of SrS and BaS; B (CaS) > B (SrS) > B (BaS); *i.e.* in inverse sequence to a_0 in agreement with the well-known relationship between B and the lattice constants: $B \propto V_0^{-1}$, where V_0 is the unit cell volume. Furthermore, the values of the calculated bulk modulus using both approximations decrease in going from CaS, to SrS, and to BaS suggesting that the compressibility increases from CaS, to SrS, and to BaS. Usually, in the treatment of alloys where the experimental data are rare, it is assumed that the atoms are located at the ideal lattice sites and the lattice constant varies linearly with composition x according to the Vegard's law [22].

$$a\left(A_xB_{1-x}C\right) = xa_{AC} + \left(1-x\right)a_{BC} \qquad (2)$$

where a_{AC} and a_{BC} are the equilibrium lattice constants of the binary compounds AC and BC respectively, $a(A_x B_{1-x} C)$ is the alloy lattice constant. However, variation of Vegard's law has been observed in semiconductor alloys both experimentally [23] and theoretically [24-28]. Hence, the lattice constant can be written as:

$$a\left(A_xB_{1-x}C\right) = xa_{AC} + \left(1-x\right)a_{BC} - x\left(1-x\right)b \qquad (3)$$

where the quadratic term b is the bowing parameter. **Figures 1(a)-(c)** and **2(a)-(c)** show the variation of the calculated equilibrium lattice constant and bulk modulus as a function of concentrations x for $Sr_xCa_{1-x}S$, $Ba_xCa_{1-x}S$ and $Ba_xSr_{1-x}S$ alloys. The obtained results for the composition dependence of the calculated equilibrium lattice parameter exhibit an agreement with Vegard's law [22]. In going from CaS, SrS and BaS; when the Sr and Ba-content increases, the values of the lattice parameters of the $Sr_xCa_{1-x}S$, $Ba_xCa_{1-x}S$, $Ba_xSr_{1-x}S$ alloys increases. Oppositely, one can see from **Figure 2** that the value of the bulk modulus increases with the decrease of Sr and Ba concentrations. The bowing parameters are determined by a polynomial fit. From **Tables 3(a)-(c)**, both approxiations follow the tendency demonstrated by both experimental measurement and theoretical calculations.

3.2. Electronic Properties

The calculated band structure energies for binary compounds as well as their investigated alloys using FP-LMTO within both LDA and GGA schemes yields indirect band gap (Γ→X) for the binary compounds of CaS, SrS and BaS. When the composition x varies, the valence band maximum (VBM) and the conduction band minimum (CBM) occur at the Γ-point, resulting in direct band gap (Γ→Γ) for the studied alloys. The calculated direct band gap (Γ→Γ) values for $Sr_xCa_{1-x}S$, $Ba_xCa_{1-x}S$ and $Ba_xSr_{1-x}S$ alloys are listed in **Table 4**, along with the available theoretical and experimental results. The computed direct band gaps for the binary compounds are in good agreements with other results. For SrS and CaS compounds, the calculated band gap is smaller than the experimental value but for the BaS is the opposite. To the

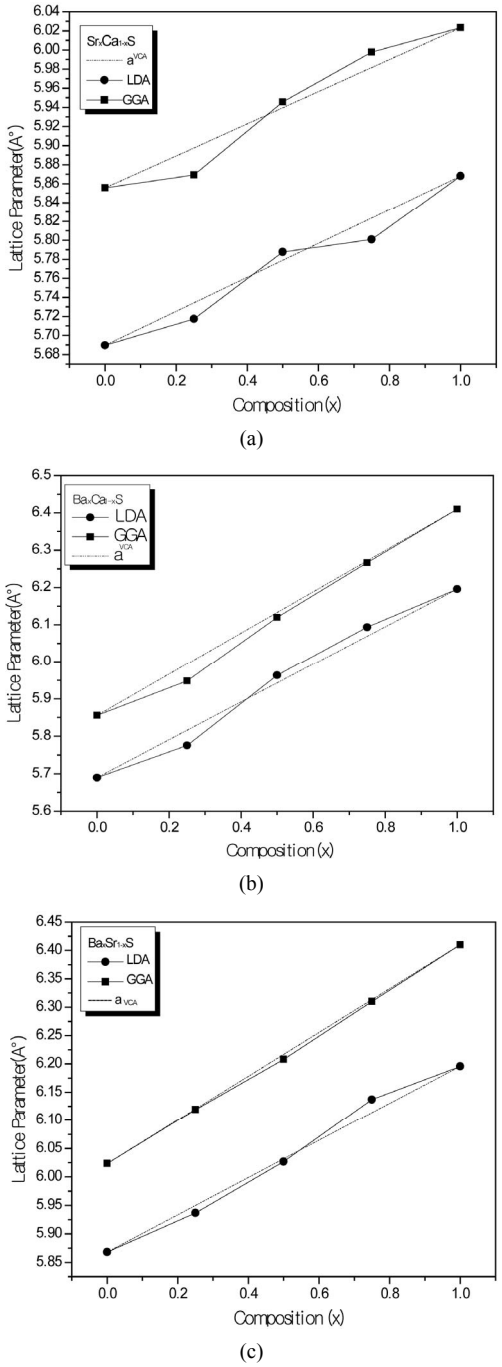

Figure 1. Composition dependence of the calculated lattice constants within GGA (solid squares) and LDA (solid circle) of (a) $Sr_xCa_{1-x}S$; (b) $Ba_xCa_{1-x}S$, (c) $Ba_xSr_{1-x}S$ alloys compared with Vegard's prediction (dot line).

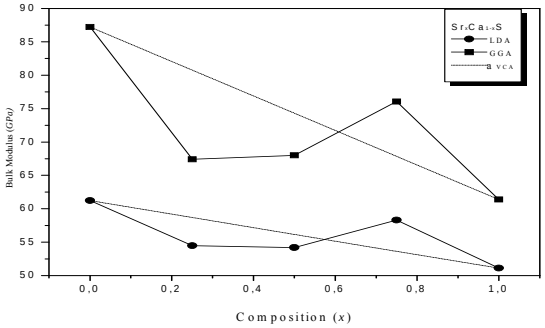

(a)

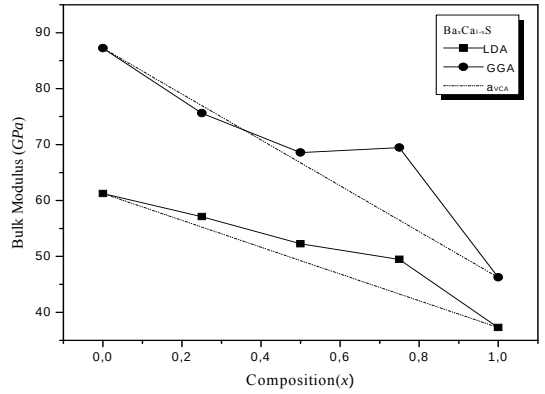

(b)

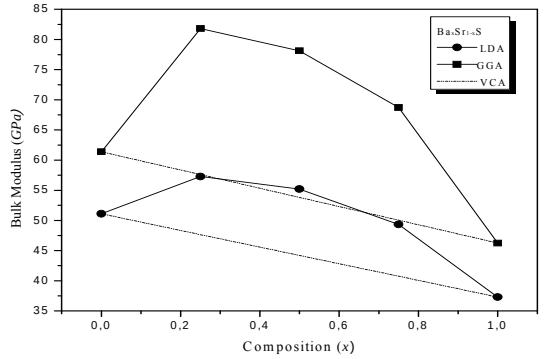

(c)

Figure 2. Composition dependence of the calculated bulk modulus within GGA (solid circle) and LDA (solid squares) of (a) $Sr_xCa_{1-x}S$; (b) $Ba_xCa_{1-x}S$; (c) $Ba_xSr_{1-x}S$ alloys compared with Vegard's prediction (dot line).

best of our knowledge, there are no theoretical or experimental data on the energy band gaps for $x = 0.25$, 0.5 and 0.75 available in literature to make a meaningful comparison. It is worthy to mention here that both LDA and GGA do not reproduce a perfect agreement with the experimental results because they do not take into account the quasi particle self energy correctly [32] that make them not sufficiently flexible to accurately reproduce both the exchange-correlation energy and its charge derivative. It is important to note that the density functional formalism is limited [30] and the derived band

Table 3. Decomposition of optical bowing into volume deformation (VD), charge exchange (CE) and structural relaxation (SR) contributions (all values in eV) for (a) $Sr_xCa_{1-x}S$; (b) $Ba_xCa_{1-x}S$; (c) $Ba_xSr_{1-x}S$.

(a)

		This work	
		LDA	GGA
x			
0.25	b_{VD}	0.0289	–7.0267
	b_{CE}	0.3231	7.2559
	b_{SR}	0.1191	0.1390
	b	0.4711	–0.3682
0.5	b_{VD}	0.0028	–5.16847
	b_{CE}	0.2053	5.2978
	b_{SR}	0.0459	0.8105
	b	0.2540	–0.9398
0.75	b_{VD}	0.0182	–5.3340
	b_{CE}	0.0577	5.1799
	b_{SR}	0.1529	–0.0847
	b	0.1924	–0.2388

(b)

		This work	
		LDA	GGA
x			
0.25	b_{VD}	–0.0690	0.2253
	b_{CE}	1.9333	1.1696
	b_{SR}	0.4386	–0.2958
	b	2.3029	1.0991
0.5	b_{VD}	–0.7494	0.1580
	b_{CE}	1.1470	0.3805
	b_{SR}	0.2729	0.0689
	b	0.6705	0.6074
0.75	b_{VD}	–1.1323	–0.6571
	b_{CE}	0.2351	1.0568
	b_{SR}	–0.1497	–2.3467
	b	–1.0469	–1.9470

(c)

		This work	
		LDA	GGA
x			
0.25	b_{VD}	0.0472	0.0030
	b_{CE}	0.7029	0.3447
	b_{SR}	0.1220	0.0085
	b	0.8721	0.3562
0.5	b_{VD}	0.0515	0.0036
	b_{CE}	0.3501	0.9317
	b_{SR}	0.0364	–0.7850
	b	0.4380	0.1503
0.75	b_{VD}	0.0044	0.0035
	b_{CE}	0.0896	–0.0957
	b_{SR}	–0.1342	0.0
	b	–0.0402	–0.092

Table 4. Direct and indirect band gap energy of $Sr_xCa_{1-x}S$, $Ba_xCa_{1-x}S$ and $Ba_xSr_{1-x}S$ at different CaS, SrS and BaS concentrations (all values are in eV).

Compounds	Energy gap (eV)	
	(Γ– Γ)	(Γ–X)
SrS		
LDA	3.871	1.931
GGA	3.685	2.294
Expt	4. 32[e]	
Others	2.45[f], 2.68[d], 3.51[d], 3.58[b]	2.25[e], 2.45[a], 2.16[e], 3.31[e]
CaS		2.3[d], 2.56[b]
LDA	3.969	2.115
GGA	3.863	2.480
Expt	4.13[e]	
Others	2.39[a], 2.4[e]	3.2[e],1.9[c], 2.5[g], 2.1[c]
BaS		
LDA	3.721	1.732
GGA	3.685	2.084
Expt	1.732	
Others		
$Sr_{0.25}Ca_{0.75}S$		
LDA	1.981	2.350
GGA	2.365	2.692
Others	2.1[c] , 2.4[c] , 2.2[c]	
$Sr_{0.5}Ca_{0.5}S$		
LDA	1.983	2.400
GGA	2.152	2.540
Others	2.2[c] , 2.4[c] 2.3[c]	
$Sr_{0.75}Ca_{0.25}S$		
LDA	1.941	2.286
GGA	2.385	2.693
Others	2.45[c] , 2.5[c] , 2.4[c]	
$Ba_{0.25}Ca_{0.75}S$		
LDA	1.557	1.703
GGA	2.175	2.316
$Ba_{0.5}Ca_{0.5}S$		
LDA	1.610	1.801
GGA	2.134	2.292
$Ba_{0.75}Ca_{0.25}S$		
LDA	1.791	1.914
GGA	2.152	2.276
$Ba_{0.25}Sr_{0.75}S$		
LDA	1.718	1.703
GGA	2.175	2.316
$Ba_{0.5}Sr_{0.5}S$		
LDA	1.722	1.801
GGA	2.151	2.316
$Ba_{0.75}Sr_{0.25}S$		
LDA	1.789	1.914
GGA	2.154	2.316

[a]Ref. [34]. [b]Ref. [39] .[c]Ref. [42]. [d]Ref. [43]. [e]Ref [44]. [f]Ref. [45]. [g]Ref. [46]

structure can't be used directly for comparison with experiment. We also mention, it is far to say that the experimental data are well reproduced by calculations. On For this reason for this that the theory holds applies pertains at $T = 0$ K, whereas the experimental measurements were performed at room temperature where the lattice vibrations are present.

The variation of the composition (x) versus the direct (Γ→Γ) and indirect (Γ→X) band gaps with both LDA and GGA approximations is shown in **Figures 3(a)-(c)**. According to this figure we notice that for concentrations (x) ranging from $x = 0.224$ to 0.769 LDA, $x = 0.216$ to 0.784 GGA the alloy exhibits a direct band gap (Γ→Γ) for both approximations $Sr_xCa_{1-x}S$, from $x = 0.26$ to 0.73 LDA, $x = 0.25$ to 0.73 GGA the alloy exhibits a direct band gap (Γ→Γ) for both approximations $Ba_xSr_{1-x}S$, from $x = 0.27$ to 0.73 LDA, $x = 0.25$ to 0.73 GGA the alloy exhibits a direct band gap (Γ→Γ) for both approximations $Ba_xSr_{1-x}S$,. It is also seen that the direct and indirect band gaps show a nonlinear behaviour with increasing Strontium, Calcium and Baryum concentrations providing a positive and negative band gap bowing for the direct (Γ→Γ) and indirect (Γ→X) band gaps, respectively. Indeed, it is a general trend to describe the band gap of $A_xB_{1-x}C$ alloys in terms of the binary compounds energy gaps E_{AC} and E_{BC} by the following semi-empirical formula:

$$E_g(x) = xE_{AC} + (1-x)E_{BC} - bx(1-x) \quad (4)$$

where E_{AC} and E_{BC} corresponds to the energy gap of SrS and CaS for the $Sr_xCa_{1-x}S$ alloy. From **Table 4**, it is clear that E_g of LDA is slightly larger than those of GGA.

The calculated band gap versus concentration was fitted by a polynomial equation. The results are shown in **Figure 3** and are summarized as follows:

$$Sr_xCa_{1-x}S \rightarrow \begin{cases} E_{\Gamma-\Gamma} = 3.90 - 8.99x + 8.91x^2 & (\text{LDA}) \\ E_{\Gamma-\Gamma} = 3.82 - 7.04x + 6.91x^2 & (\text{GGA}) \\ E_{\Gamma-X} = 2.11 + 1.36x - 1.54x^2 & (\text{LDA}) \\ E_{\Gamma-X} = 2.48 + 0.90x - 1.05x^2 & (\text{GGA}) \end{cases} \quad (5)$$

$$Ba_xCa_{1-x}S \rightarrow \begin{cases} E_{\Gamma-\Gamma} = 3.84 - 10.18x + 10.07x^2 & (\text{LDA}) \\ E_{\Gamma-\Gamma} = 3.81 - 7.57x + 7.42x^2 & (\text{GGA}) \\ E_{\Gamma-X} = 2.03 - 0.77x - 0.54x^2 & (\text{LDA}) \\ E_{\Gamma-X} = 2.45 - 0.28x - 0.057x^2 & (\text{GGA}) \end{cases} \quad (6)$$

$$Ba_xSr_{1-x}S \rightarrow \begin{cases} E_{\Gamma-\Gamma} = 3.79 - 9.50x + 9.41x^2 & (\text{LDA}) \\ E_{\Gamma-\Gamma} = 3.65 - 6.98x + 6.97x^2 & (\text{GGA}) \\ E_{\Gamma-X} = 1.91 + 0.15x - 0.30x^2 & (\text{LDA}) \\ E_{\Gamma-X} = 2.28 + 0.37x - 0.55x^2 & (\text{GGA}) \end{cases} \quad (7)$$

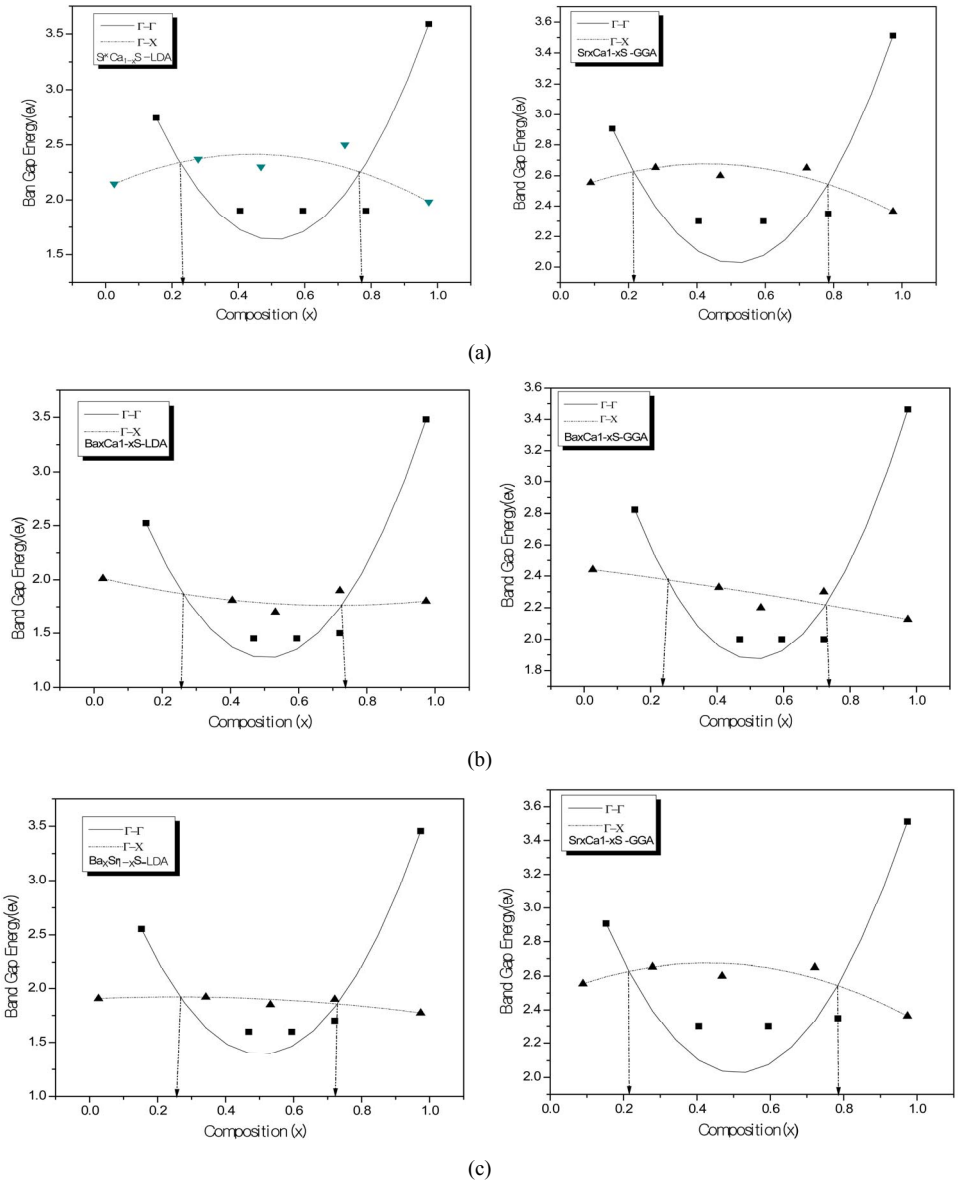

Figure 3. The calculated direct (Γ→Γ) and indirect (Γ→X) band gaps of (a) $Sr_xCa_{1-x}S$ alloy as a function of Sr, Ca, and concentrations using LDA (a) and GGA (b) schemes; (b) $Ba_xCa_{1-x}S$, as a function of Ba and Ca concentrations using LDA (a) and GGA (b) schemes; (c) $Ba_xSr_{1-x}S$ alloy as a function of Ba and Sr concentrations using LDA (a) and GGA (b) schemes.

In order to understand the physical origins of bowing parameters in $A_xB_{1-x}C$ alloy, we follow the procedure of Bernard and Zunger [31], and decompose the total bowing parameter b into physically distinct contributions. The overall bowing coefficient at a given average composition x measures the change in the band gap according to the formal reaction.

$$xAC\left(a_{AC}\right)+\left(1-x\right)BC\ \left(a_{BC}\right)\rightarrow A_xB_{1-x}C\left(a_{eq}\right) \quad (6)$$

where a_{AC} and a_{BC} are the equilibrium lattice constants of the binary compounds and a_{eq} is the equilibrium lattice constant of the alloy with the average composition x.

Equations (5)-(7) are decomposed into three steps:

$$AC\left(a_{AC}\right)+BC\left(a_{BC}\right)\rightarrow AC\left(a\right)+BC\left(a\right) \quad (8)$$

$$xAC\left(a\right)+\left(1-x\right)BC\ \left(a\right)\rightarrow A_xB_{1-x}C\left(a\right) \quad (9)$$

$$A_xB_{1-x}C\left(a\right)\rightarrow A_xB_{1-x}C\left(a_{eq}\right) \quad (10)$$

The first step attributes the volume deformation (VD) effect on the bowing. The corresponding contributions b_{VD} to the bowing parameter represents the relative response of the band structure of the binary compounds AC and BC to hydrostatic pressure that arises from the change of their individual equilibrium lattice constants to

the alloy value $a = a(x)$. The second contribution, the charge exchange (CE) contribution b_{CE}, reflects a charge transfer effect which is due to different (averaged) bonding behaviour of at the lattice constant a. The final step, the structural relaxation (SR), reflects changes in passing from the unrelaxed to the relaxed alloy by b_{SR}. Consequently, the total bowing parameter is defined as.

$$b = b_{VD} + b_{CE} + b_{SR} \quad (11)$$

The general representation of the composition-dependent band gap of the alloys in terms of binary compounds energy gaps of the, $E_{AC}(a_{AC})$ and $E_{BC}(a_{BC})$, and the total bowing parameter b is

$$E_g(x) = xE_{AC}(a_{AC}) + (1-x)E_{BC}(a_{BC}) - bx(1-x) \quad (12)$$

This allows a division of the total bowing b into three contributions according to:

$$b_{VD} = \frac{E_{AC}(a_{AC}) - E_{AC}(a)}{1-x} + \frac{E_{BC}(a_{BC}) - E_{BC}(a)}{x} \quad (13)$$

$$b_{CE} = \frac{E_{AC}(a)}{1-x} + \frac{E_{BC}(a)}{x} - \frac{E_{ABC}(a)}{x(1-x)} \quad (14)$$

$$b_{SR} = \frac{E_{ABC}(a) - E_{ABC}(a_{eq})}{x(1-x)} \quad (15)$$

All these energy gaps mentioned in (13)-(15) have been calculated for the indicated atomic structures and lattice constants. **Table 3(a)** shows the calculated optical band gap bowing b for $Sr_xCa_{1-x}S$ for three different molar fractions (x = 0.25, 0.5 and 0.75). The LDA (GGA) calculated band gap bowing (b) is found to be equal to –0.3185 (–0.7746) eV, 0.078 (0.0214) eV and 4.0222 (3.6608) eV for x = 0.25, 0.5 and 0.75 respectively. From **Table 3(a)** we notice that the structural relaxation effect is negligible for the studied compositions x = 0.25, 0.50 and 0.75 and the main contribution to the band gap bowing is essentially due to the charge exchange (CE) contribution, for x = 0.75 the band gap bowing is due to nearly equal contribution of the volume deformation (SR) effects. **Table 3(b)** shows the calculated optical band gap bowing b for $Ba_xCa_{1-x}S$ for three different molar fractions (x = 0.25, 0.5 and 0.75). The LDA (GGA) calculated band gap bowing (b) is found to be equal to 2.3029 (1.0991) eV, 0.6705 (0.6074) eV and –1.0469 (–1.947) eV for x = 0.25, 0.5 and 0.75 respectively. From **Table 3(b)** we notice that the structural relaxation effect is negligible for the studied compositions x = 0.25, 0.50 and 0.75 and the main contribution to the band gap bowing is essentially due to the charge exchange (CE) contribution, for x = 0.25 and 0.5. For x = 0.75 the band gap bowing is due to nearly equal contribution of the volume deformation (VD) effects. **Table 3(c)** shows the calculated optical band gap bowing b for $Ba_xSr_{1-x}S$ for three different molar fractions (x = 0.25, 0.5 and 0.75). The LDA (GGA) calculated band gap bowing (b) is found to be equal to 0.8721 (0.3562) eV, 0.438 (0.1503) eV and –0.0402 (–0.0922) eV for x = 0.25, 0.5 and 0.75 respectively. From **Table 3(c)** we notice that the structural relaxation effect is negligible for the studied compositions x = 0.25, 0.50 and 0.75 and the main contribution to the band gap bowing is essentially due to the charge exchange (CE) contribution for x = 0.25 and 0.5. For x = 0.75 the band gap bowing is due to nearly equal contribution of the volume deformation (SR) effects. **Figure 4(a)** shows the variation of the band gap bowing versus concentration. It is shown that the optical bowing remains linear and increases slowly in going from 0.25 to 0.75, for LDA and for GGA it remains linear varies rapidly in going from 0.25 to 0.5, and beyond 0.5 it increases rapidly too, which confirms the evaluation of the band gap according to the concentration,. **Figure 4(b)** for $Ba_xCa_{1-x}S$ shows the variation of the band gap bowing versus concentration. It is shown that the optical bowing remains linear (in going) from 0.25 to 0.75 for LDA and for GGA it remains linear with a tow slope varying slowly (in going) from 0.25 to 0.5, and beyond 0.5 it decreases rapidly. **Figure 4(c)** for $Ba_xSr_{1-x}S$ shows the variation of the band gap bowing versus concentration. It is shown that the optical bowing remains linear, it monotonicly decreases from 0.25 to 0.75 both for LAD, GGA with two slopes. To the best of our knowledge, there are no theoretical or experimental data on the band gap bowing to compare with our predicted results.

3.3. Effective Masses

Knowledge of the electron and hole effective mass values is indispensable for the understanding of transport phenomena, exciton effects and electron-hole in semiconductors. Excitonic properties are of great interest for semiconductor materials; therefore, it is worthwhile to estimate the electron and hole effective mass values for $Sr_xCa_{1-x}S$, $Ba_xCa_{1-x}S$ and $Ba_xSr_{1-x}S$ alloys at different compositions. Experimentally, the effective masses are usually determined by cyclotron resonance, electro reflectance measurements or from the analysis of transport data or transport measurements [32]. Theoretically, the effective masses can be estimated from the energy band curvatures. Generally, the effective mass is a tensor with nine components, however for the much idealized simple case, where the E-k diagram can be fitted by a parabola $E = \hbar^2 k^2 / 2m^*$, the effective mass becomes a scalar at high symmetry point in Brillouin zone. We have computed the electron effective mass at the conduction band minima (CBM) and the hole effective mass at the valence

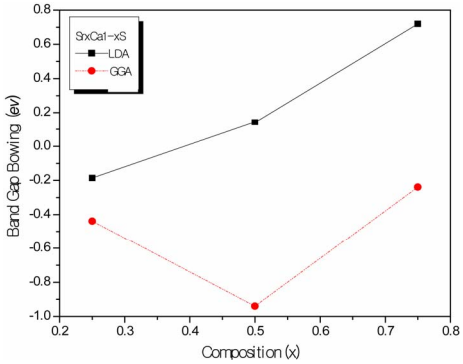

(a)

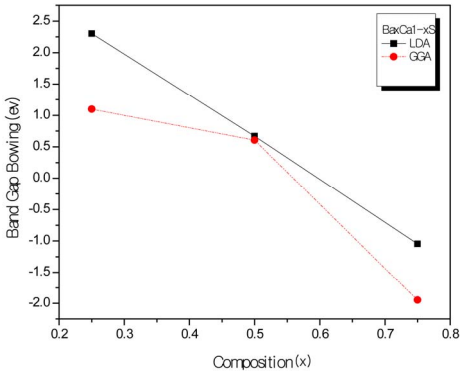

(b)

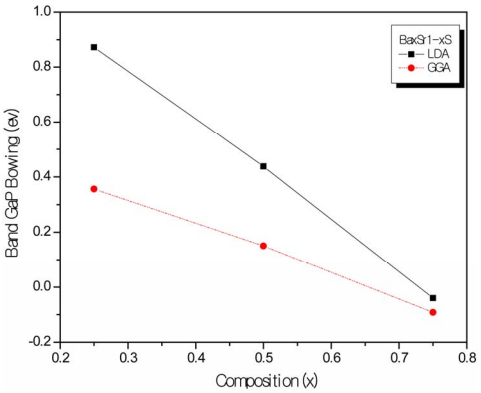

(c)

Figure 4. The calculated optical bowing parameters as a function of (a) Sr and Ca; (b) Ba and Ca; (c) Ba and Sr, concentrations within LDA and GGA schemes.

band maxima (VBM) for the composition ranging from 0 to 1.0 for $Sr_xCa_{1-x}S$, $Ba_xCa_{1-x}S$ and $Ba_xSr_{1-x}S$ alloys. The electron effective mass value are obtained from the curvature of the conduction band near the X-point for SrS ,BaS and CaS and near the Γ-point at the CBM for X = 0.25, 0.5 and 0.75. The hole effective masse value is calculated from the curvature near the Γ-point at the VBM for all concentration. The calculated electron and hole effective mass values for for $Sr_xCa_{1-x}S$, $Ba_xCa_{1-x}S$ and $Ba_xSr_{1-x}S$ alloys are mentioned in **Tables 5(a)-(c)**.

Table 5. Electron (m_e^*), heavy hole (m_{hh}^*) and light hole (m_{lh}^*) effective masses (in units of free electron mass m_0) of the ternary (a) $Sr_xCa_{1-x}S$; (b) $Ba_xCa_{1-x}S$; (c) $Ba_xSr_{1-x}S$ alloy using LDA and GGA schemes.

(a)

	m_e^*		m_{hh}^*		m_{lh}^*	
x	LDA	GGA	LDA	GGA	LDA	GGA
1	0.101	0.110	1.380	1.290	0.360	0.547
0.25	0.200	0.210	2.410	3.530	6.690	8.870
0.5	0.220	0.240	4.050	5.220	6.810	8.670
0.75	0.290	0.230	3.280	4.430	5.520	7.480
0	0.150	0.160	0.490	0.600	0.940	1.150

(b)

	m_e^*		m_{hh}^*		m_{lh}^*	
x	LDA	GGA	LDA	GGA	LDA	GGA
1	0.102	0.109	1.110	2.510	1.650	2.930
0.25	0.250	0.260	1.007	1.610	0.102	0.190
0.5	0.290	0.315	1.609	2.350	0.390	0.640
0.75	0.270	0.310	2.140	3.020	0.490	1.020
0	0.150	0.160	0.490	0.600	0.940	1.150

(c)

	m_e^*		m_{hh}^*		m_{lh}^*	
x	LDA	GGA	LDA	GGA	LDA	GGA
1	0.102	0.109	1.110	2.510	1.650	2.930
0.25	0.216	0.220	2.180	3.360	2.180	1.190
0.5	0.310	0.250	1.930	2.890	1.710	1.240
0.75	0.258	0.258	3.100	3.100	1.090	1.390
0	0.101	0.110	1.380	1.290	0.940	1.150

4. Conclusions

The (FP-LMTO) method is used to calculate the structural and electronic properties of the rocksalt SrS, CaS, BaS and their $Sr_xCa_{1-x}S$, $Ba_xCa_{1-x}S$ and $Ba_xSr_{1-x}S$ alloys.From this, we may conclude that:

1) The variation of the structural parameters with Sr, Ca and Ba concentrations obeys Vegard's law.

2) The electronic band structure shows a non-linear variation of the fundamental band gaps versus Sr, Ca and Ba concentrations. The deviation from linearity is characterized by a calculated optical bowing parameter. The main contribution to the optical bowing is essentially due to volume deformation effects.

3) The effective masses indicate that the charge carri-

ers in these alloys should be dominated by electrons.

REFERENCES

[1] S. Labidia, H. Meradji, M. Labidia, S. Ghemid, S. Drablia and F. El H. Hassan, "First Principles Calculations of Structural, Electronic and Thermodynamic Properties of SrS,SrSe,SrTe Compounds and $SrS_{1-x}Se_x$ Alloy", *Physics Procedia*, Vol. 2, No. 3, 2009, pp. 1205-1212. doi:10.1016/j.phpro.2009.11.083

[2] M. A. Haase, J. Qiu, J. M. DePuydt and H. Cheng, "Blue-Green Laser Diodes," *Applied Physics Letters*, Vol. 59, No. 11, 1991, p. 1272.

[3] A. Yamasaki and T. Fujiwara, "Electronic Structure of Oxides MO (M = Mg, Ca, Ti, V) in the GW Approximation," *Physical Review B*, Vol. 66, 2002, Article ID: 245108.

[4] Z. Charifi, H. Baaziz, F. El H. Hassan and N. Bouarissa, "High Pressure Study of Structural and Electronic Properties of Calcium Chalcogenides," *Journal of Physics*: *Condensed Matter*, Vol. 17, No. 26, 2005, p. 4083. doi:10.1088/0953-8984/17/26/008

[5] V. Wagner, *et al*., "Lattice Dynamics and Bond Polarity of Be-Chalcogenides A New Class of II-VI Materials," *Physica Status Solidi B*, Vol. 215, No. 1, 1999, pp. 87-91. doi:10.1002/(SICI)1521-3951(199909)215:1<87::AID-PSSB87>3.0.CO;2-D

[6] Y. Nakanishi, T. Ito, Y. Hatanaka and G. Shimaoka, "First-Principles Study of Structural, Electronic and Optical Properties of $SrS_{1-x}Se_x$ Alloys," *Applied Surface Science*, Vol. 65-66, 1992, pp. 515-519. doi:10.1016/0169-4332(93)90712-K

[7] S. Asano, N. Yamashita and Y. Nakao, "Luminescence of the Pb^{2+}-Ion Dimer Center in CaS and CaSe Phosphors," *Physica Status Solidi B*, Vol. 89, No. 2, 1978, pp. 663-673. doi:10.1002/pssb.2220890242

[8] R. Pandey and S. Sivaraman, "Spectroscopic Properties of Defects in Alkaline-Earth Sulfides," *Journal of Physics and Chemistry of Solids*, Vol. 52, No. 1, 1991, pp. 211-225.

[9] Ö. Akinci, H. H. Gürel and H. Ünlü, "Semi-Empirical Tight Binding Modelling of CdSTe/CdTe, ZnSSe/ZnSe and ZnSSe/CdSe Heterostructures," *Thin Film Chalogenide Photovoltaic Materials*, Vol. 517, No. 7, 2009, pp. 2431-2437.

[10] H. Morko, C. H. UnlU and G. Ji, "Principles & Technology of MODFETs," Wiley, New York, 1991.

[11] "Thin Film Chalcogenide Photovoltaic Materials," In: R. Scheer, J.-F. Guillemoles, A. N. Tiwari, *et al*., Eds., *Society Symposium Proceedings on Ferekides European Materials Research*, 2008.

[12] A. Zunger, S.-H. Wei, L. G. Ferreira and J. E. Bernard, "Special Quasirandom Structures," *Physical Review Letters*, Vol. 65, No. 3, 1990, pp. 353-356. doi:10.1103/PhysRevLett.65.353

[13] S. Savrasov and D. Savrasov, "Full-Potential Linear-Muffin-Tin-Orbital Method for Calculating Total Energies and Forces," *Physical Review B*, Vol. 46, 1992, pp. 2181-2195.

[14] S. Y. Savrasov, "Linear-Response Theory and Lattice Dynamics: A Muffin-Tin-Orbital Approach," *Physical Review B*, Vol. 54. 1996, pp. 16470-16486.

[15] P. Hohenberg and W. Kohn, "Inhomogeneous Electron GaS," *Physical Review*, Vol. 136, 1964, pp. B864-B871

[16] W. Kohn and L. J. Sham, "Self-Consistent Equations Including Exchange and Correlation Effects," *Physical Review*, Vol. 140, No. 4A, 1965, pp. 1133-1138. doi:10.1103/PhysRev.140.A1133

[17] S. Y. Savrasov, "Program LMTART for Electronic Structure Calculations", *Zeitschrift fur Kristallographie*, Vol. 220, No. 5-6, 2005, pp. 555-557. doi:10.1524/zkri.220.5.555.65067

[18] J. P. Perdew and Y. Wang, "Pair-Distribution Function and Its Coupling-Constant Average for the Spin-Polarized Electron Gas," *Physical Review B*, Vol. 46, No. 20, 1992, pp. 12947-12954. doi:10.1103/PhysRevB.46.12947

[19] J. P. Perdew, S. Burke and M. Ernzerhof, "Generalized Gradient Approximation Made Simple," *Physical Review Letters*, Vol.77, No. 18, 1996, pp. 3865-3868.

[20] P. Blochl, O. Jepsen and O. K. Andersen, "Improved Tetrahedron Method for Brillouin-Zone Integrations," *Physical Review B*, Vol. 49, No. 23, 1994, pp. 16223-16233. doi:10.1103/PhysRevB.49.16223

[21] F. D. Murnaghan, "The Compressibility of Media under Extreme Pressures," *Proceedings of the National Academy of Sciences USA*, Vol. 30, 1944, pp. 244-247. doi:10.1073/pnas.30.9.244

[22] L. Vegard, "Formation of Mixed Crystals by Solid-Phase Contact", *Zeitschrift fur Kristallographie*, Vol. 5, No. 5, 1921, pp. 393-395. doi:10.1007/BF01327675

[23] B. Jobst, D. Hommel, U. Lunz, T. Gerhard and G. Landwehr, "E_0 Band-Gap Energy and Lattice Constant of Ternary $Zn_{1-x}Mg_xSe$ as Functions of Composition," *Applied Physics Letters*, Vol. 69, No. 1, 1996, pp. 97-100. doi:10.1063/1.118132

[24] F. El H. Hassan and H. Akbardadeh, "First-principles Investigation of BN_xP_{1-x}, BN_xAs_{1-x} and BP_xAs_{1-x} Ternary Alloys," *Materials Science and Engineering B*, Vol. 121, No. 1-2, 2005, pp. 170-177. doi:10.1016/j.mseb.2005.03.019

[25] Y. Al-Douri, "Structural Phase Transition of Boron Nitride Compound," *Solid State Communications*, Vol. 132, No. 7, 2004, pp. 465-470. doi:10.1016/j.ssc.2004.08.020

[26] Y. Al-Douri, "Electronic and Positron Properties of Zinc-Blende Structure of GaN, AlN, and Their Alloy $Ga_{1-x}Al_xN$," *Journal of Applied Physics*, Vol. 93, No. 12, 2003, pp. 9730-9736. doi:10.1063/1.1573739

[27] Y. Al-Douri, "Electronic and Optical Properties of $Zn_xCd_{1-x}Se$," *Materials Chemistry and Physics*, Vol. 82, No. 1, 2003, pp. 49-54.

[28] Y. Al-Douri, S. Mecabih, N. Benosman and H. Aourag, "Pressure Effect on Electronic and Positron Charge Densities of $Zn_{0.5}Cd_{0.5}Se$," *Physica B*, Vol. 325, No. 1-4, 2003, pp. 362-371.

[29] S. N. Rashkeev and W. R. L. Lambrecht, "Second-Harmonic Generation of I-III-VI_2 Chalcopyrite Semiconductors: Effects of Chemical Substitutions," *Physical Review B*, Vol. 63, No. 16, 2001, Article ID: 165212.

[30] G. Onida, L. Reining and A. Rubio, "Electronic Excitations: Density-Functional versus Many-Body Green's-Function Approaches," *Reviews of Modern Physics*, Vol. 74, No. 2, 2002, pp. 601-659.

[31] J. E. Bernard and A. Zunger, "Electronic Structure of ZnS, ZnSe, ZnTe, and Their Pseudobinary Alloys," *Physical Review B*: *Condens Matter*, 1987, pp. 3199-3228.

[32] O. Zakharov, A. Rubio, X. Blase, M. L. Cohen and S. G. Louie, "Quasiparticle Band Structures of Six II-VI Compounds: ZnS, ZnSe, ZnTe, CdS, CdSe, and CdTe," *Physical Review B*, Vol. 50, No. 15, 1994, pp. 10780-10787. doi:10.1103/PhysRevB.50.10780

[33] K. Syassen, "Pressure-Induced Structural Transition in SrS," *Physica Status Solidi* (*A*), Vol. 91, No. 1, 1985, pp. 11-15. doi:10.1002/pssa.2210910102

[34] R. Khenata, H. Baltache, M. Rerat, M. Driz, M. Sahnoun, B. Bouhafs and B. Abbar, "First-Principle Study of Structural, Electronic and Elastic Properties of SrS, SrSe and SrTe under Pressure," *Physica B*: *Physics of Condensed Matter*, Vol. 339, No. 4, 2003, pp. 208-215. doi:10.1016/j.physb.2003.07.003

[35] P. Cartona and P. Masri, "Cohesive Properties and Behaviour under Pressure of CaS, CaSe, and CaTe: Results of *ab Initio* Calculations," *Journal of Physics*: *Condensed Matter*, Vol. 10, No. 40, 1998, pp. 8947-8955. doi:10.1088/0953-8984/10/40/003

[36] Z. Charifi, H. Baaziz, F. El H. Hassan and N. Bouarissa, "High Pressure Study of Structural and Electronic Properties of Calcium Chalcogenides," *Journal of Physics*: *Condensed Matter*, Vol. 17, No. 26, 2005, p. 4083. doi:10.1088/0953-8984/17/26/008

[37] A. Bouhemadou, R. Khenata, F. Zegrar, M. Sahnoun, H. Baltache and A. H. Reshak, "*Ab Initio* Study of Structural, Electronic, Elastic and High Pressure Properties of Barium Chalcogenides," *Computational Materials Science*, Vol. 38, No. 2, 2006, pp. 263-270. doi:10.1016/j.commatsci.2006.03.001

[38] S. Drablia, H. Meradji, S. Ghemid, G. Nouet and F. El H. Hassan, "First Principles Investigation of Barium Chalcogenide Ternary Alloys," *Computational Materials Science*, Vol. 46, No. 2, 2009, pp. 376-382. doi:10.1016/j.commatsci.2009.03.013

[39] I. B. S. Banu, M. Rajagopalan, B. Palanivel, G. Kalpana, P. Shenbagaraman and J. L. Temp, "Structural and Electronic Properties of SrS, SrSe, and SrTe under Pressure," *Physics*, Vol. 112, No. 3-4, 1998, pp. 211-226.

[40] S. Labidi, H. Meradji, S. Ghemid, M. Labidi and F. El H. Hassan, "FP-LAPW Investigations of $SrS_{1-x}Se_x$, $SrS_{1-x}Te_x$ and $SrSe_{1-x}Te_x$ Ternary Alloys," *Journal of Physics*: *Condensed Matter*, Vol. 20, No. 44, 2008, Article ID: 445213. doi:10.1088/0953-8984/20/44/445213

[41] S. Ekbundit, A. Chizmeshya, R. LaViolette and G. H. Wolf, "Experimental and Theoretical Investigation of the High-Pressure Behavior of CaS and MgS," *Journal of Physics*: *Condensed Matter*, Vol. 8, No. 43, 1996, pp. 8251-8265. doi:10.1088/0953-8984/8/43/018

[42] A. Shaukat ,Y. Saeed, S. Nazir, N. Ikram and M. Tanveer, "*Ab Initio* Study of Structural, Electronic and Optical Properties of $Ca_{1-x}Sr_xS$ Compounds," *Physica B*: *Physics of Condensed Matter*, Vol. 404, No. 21, 2009, pp. 3964-3972. doi:10.1016/j.physb.2009.07.147

[43] Y. Kaneko and T. Koda, "New Developments in IIa-VIb (Alkaline-Earth Chalcogenide) Binary Semiconductors," *Journal of Crystal Growth*, Vol. 86, No. 1-4, 1990, pp. 72-78. doi:10.1016/0022-0248(90)90701-L

[44] S. Yamaoka, O. Shimomura, H. Nakazawa and O. Fukunaga, "Pressure-Induced Phase Transformation in BaS," Vol. 33, No. 1, 1980, pp. 87-89.

[45] G. B. Bachelet and N. E. Christensen, "Relativistic and Core-Relaxation Effects on the Energy Bands of Gallium Arsenide and Germanium," *Physical Review B*, Vol. 31, No. 2, 1985, pp. 879-887. doi:10.1103/PhysRevB.31.879

[46] V. S. Stepanyuk, A. Szasz, O. V. Farberovich, A. A. Grigorenko, A. V. Kozlov and V. V. Mikhailin, "An Electronic Band Structure Calculation and the Optical Properties of Alkaline-Earth Sulphides," *Physica Status Solidi B*, Vol. 155, No. 1, 1989, pp. 215-220. doi:10.1002/pssb.2221550121

